

N O T I C E

THIS DOCUMENT HAS BEEN REPRODUCED FROM
MICROFICHE. ALTHOUGH IT IS RECOGNIZED THAT
CERTAIN PORTIONS ARE ILLEGIBLE, IT IS BEING RELEASED
IN THE INTEREST OF MAKING AVAILABLE AS MUCH
INFORMATION AS POSSIBLE

80-10335

CR-163541

May 1980

DEFINING RELATIONSHIPS BETWEEN SURFACE CHARACTERISTICS AND ACTUAL EVAPORATION RATE

by: *M. Menenti*

Institute for Land and Water Management Research (I.C.W.)
Wageningen, the Netherlands

The present work was carried out while the author was on leave from TECNECO S.p.A., S. Ippolito, Pesaro, Italy. It was presented orally at the 4th Meeting of Working Group II of the TELLUS Project at Monterotondo (Roma), November 20 - 21, 1979.

(E80-10335) DEFINING RELATIOSHIPS BETWEEN
SURFACE CHARACTERISTICS AND ACTUAL
EVAPOBATION RATE (Institute for Land and
Water Management) 25 p HC A02/MF A01

N80-33834

CSCL 05B G3/43

Unclas
00335

Correspondence regarding this series of newsletters should be addressed to:

P. REINIGER

Commission of the European Communities

JOINT RESEARCH CENTRE

I-21020 Ispra (Varese) - Italy

C O N T E N T S

	page
I INTRODUCTION	1
II TAYLOR'S EXPANSION OF THE SURFACE ENERGY BALANCE EQUATION	1
a. Concept	1
b. Numerical calculation of the derivative with respect to the surface temperature	3
c. Variability of the evaporation rate as related to the other meteorological variables	5
d. Numerical calculation of the derivative with respect to the surface temperature and reflectivity	8
e. First order approximation of the $E(T_s, \alpha)$ surface	9
III NUMERICAL CALCULATION OF APPROXIMATED EVAPORATION FORMULAS	10
a. Selection of suitable experimental points	10
b. Comparison between calculated and experimental values	12
c. Effectiveness of the aerodynamic resistance	14
d. Effectiveness of the air temperature	16
e. Summary of the results	17
IV SUMMARY AND CONCLUSIONS	18
ACKNOWLEDGEMENTS	19
REFERENCES	20
LIST OF SYMBOLS	21

ABSTRACT

To assess criteria for the determination of actual evaporation by remotely sensed surface temperature, a sensitivity analysis of the energy balance equation is performed.

Constraints in the design of field experiments are specified and criteria to collect direct spot measurements of actual evaporation are formulated.

By Taylor expansion of the energy balance equation, analytical approximations are derived and fitted to experimental data. The latter are obtained by the Bowen ratio for both actual bare soil evaporation and actual transpiration from natural vegetation.

A comparison of different equations, with actual evaporation as a function only of surface albedo and surface temperature is also presented.

I. INTRODUCTION

The work contained in this note was performed while the author was on leave from TECNECO spA (Italy) for eight months, during 1979.

According to many recent references, remotely sensed surface temperature allows for a rather promising way to the estimation of actual evaporation losses from large non-homogeneous surfaces. However, plots of direct measurements of actual evaporation versus surface temperature show a substantial scatter of the points. Therefore it is not easy to define some analytical expression of the relationship between evaporation rate and surface temperature. The problem is that such a scatter is due to the interference of other independent parameters of the surface energy balance and due to the lack of some a-priori equation to relate the parameters involved.

A way to solve this problem is to derive analytical expressions by Taylor's expansion of the energy balance equation.

II. TAYLOR'S EXPANSION OF THE SURFACE ENERGY BALANCE EQUATION

a. C o n c e p t

According to the previous suggestions, it seems worthwhile to specify in a formal way the concept of relationships between evaporation rate and the different variables of the surface energy balance equation. There is however no need to establish a new relationship as it is already implicitly included in the energy balance equation at groundlevel.

$$LE = \frac{\rho_a c_a}{r_a} (T_a - T_s) + (1-\alpha)R_s + \epsilon' \sigma T_a^4 - \epsilon \sigma T_s^4 - G \quad (\text{J.cm}^{-2}.\text{day}^{-1}) \quad (1)$$

- where L = latent heat of vaporization of water (at mean air temperature) (J.g^{-1})
- E = evaporation rate ($\text{g.cm}^{-2}.\text{day}^{-1}$)
- $\rho_a c_a$ = thermal capacity of air ($\text{J.cm}^{-3}.\text{°C}^{-1}$)
- r_a = surface aerodynamic resistance (day.cm^{-1})
- T_a = air temperature (K)
- T_s = surface temperature (K)
- α = surface reflectivity
- R_s = shortwave incoming radiation ($\text{J.cm}^{-2}.\text{day}^{-1}$)
- ϵ' = air apparent emissivity
- ϵ = surface emissivity
- σ = Stephan-Boltzmann constant ($\text{J.cm}^{-2}.\text{day}^{-1}.\text{°K}^{-4}$)
- G = heat soil flux ($\text{J.cm}^{-2}.\text{day}^{-1}$)

Such an equation may be thought as a hypersurface in \mathbb{R}^7 , with the coordinate axes being E, T_a , r_a , T_s , α , R_s , G. Eq. (1) defines a general relationship between evaporation rate and the meteorological conditions at the surface level. This relationship is not subjected to any kind of constraints related to the kind of surface and/or meteorological situation. That is to say if the turbulent exchange coefficients are evaluated without restricting hypothesis. The obvious disadvantage is the extensive data requirement of this equation: comprehensive and area-spread meteorological data are needed for the evaluation of regional evaporation losses by eq. (1). To evaluate regional evaporation, using, if possible, only remotely sensed data over large areas we thus have, for practical reasons, to look for more simple relations. This is equivalent with defining functions of a degree of dimensions lower than eq. (1), for instance a line-relationship (E, T_s), or a surface-relationship like (E, T_s , α). These functions can be defined through a Taylor's expansion of eq. (1) around some physical status E^* , where $E^* \equiv f(T_s^*, \alpha^*, r_a^*, T_a^*, G^*, R_s^*)$ with a notation in \mathbb{R}^7 .

Taylor's theorem, using the vector \underline{s} as representing the point with coordinates (x_1, \dots, x_k) in \mathbb{R}^{k+1} can be written as:

$$f(s) = f(s^*) + f'(s^*)(s-s^*) + \frac{f''(s^*)(s-s^*)^2}{2!} + \dots + \frac{f^{(n-1)}(s^*)(s-s^*)^{n-1}}{(n-1)!} + R_n \quad (2)$$

where: R_n is the remainder

$f^{(i)}$ is the total i -th order derivative with respect to $s \equiv x_1, \dots, x_k$

The sum of an unlimited number of terms as in eq. (2) approximates the function f if, and only if, the remainder approaches zero as the number of terms becomes infinite. Such a series is convergent to the function f with the number of terms. Then the error in the approximation of the function f depends on such a number.

A Taylor's series can be used to approximate the function $LE = f(T_s, \alpha, r_a, T_a, G, R_s)$. For our purposes it is very convenient to use only the linear terms in eq. (2), i.e. applying only the first order derivatives. Then from eq. (2) we get:

$$E = E^* + D_{T_s} E \frac{dT_s}{ds} \underline{i}_1 \cdot \underline{i}_7 + D_\alpha E \frac{d\alpha}{ds} \underline{i}_2 \cdot \underline{i}_7 + D_{r_a} E \frac{dr_a}{ds} \underline{i}_3 \cdot \underline{i}_7 + D_{T_a} E \frac{dT_a}{ds} \underline{i}_4 \cdot \underline{i}_7 + D_G E \frac{dG}{ds} \underline{i}_5 \cdot \underline{i}_7 + D_{R_s} E \frac{dR_s}{ds} \underline{i}_6 \cdot \underline{i}_7 \quad (3)$$

where: E^* is the value of eq. (1) at $(T_s^*, \alpha^*, r_a^*, T_a^*, G^*, R_s^*)$

D_{x_i} is the partial derivative with respect to x_i

\underline{i}_j is the versor (unit vector) of axis x_j

$\underline{i}_j \cdot \underline{i}_k$ is the scalar product between the two versors (then

equal to the cos. of the angle $\hat{i}_j \hat{i}_k$)

E, E^* are in $g \cdot cm^{-2} \cdot day^{-1}$; \underline{i}_7 is the versor of \underline{E}

b. Numerical evaluation of the derivative with respect to the surface temperature

The geometrical framework in \mathbb{R}^7 can be followed further to obtain a formal expression of the relationship between E and T_s :

$$E(T_s) = \underline{E} \cdot (\underline{i}_8, \underline{i}_1) \quad (g \cdot cm^{-2} \cdot day^{-1}) \quad (4)$$

$E(T_s)$ is the projection of the vector \underline{E} on the coordinate plane $\underline{i}_0, \underline{i}_1$. Such a projection can be approximated according to eq. (1), (3):

$$E'(T_s) = E'^* - \frac{1}{L} \left(\frac{\rho_a c_a}{r_a} + 4 \epsilon \sigma T_s^3 \right) dT_s \quad (\text{g.cm}^{-2}.\text{day}^{-1}) \quad (5)$$

where: $E'(T_s)$ is the first-order approximation of $E(T_s)$ and E'^* the value with $T_s = T_s^*$

This kind of equation can be applied to fit experimental data on evaporation rate vs. surface temperature. As can be seen from eq. (5) the slope of the function $E'(T_s)$ depends on T_s (supposed to be known everywhere) and the prevailing meteorological conditions over a wide range of the surface roughness.

However, in the common range of surface temperatures, low values of the aerodynamic resistance may cause a shift from a small slope of $E'(T_s)$ to a steeper one. In Table 1 values are reported for different aerodynamic resistances, as calculated from:

$$-\frac{1}{L} \left(\frac{\rho_a c_a}{r_a} + 4 \epsilon \sigma T_s^3 \right) \quad (\text{g.cm}^{-2}.\text{day}^{-1}.\text{K}^{-1}) \quad (6)$$

$E'(T_s)$ is decreasing everywhere, since quantities inside brackets are positive, when δT_s is positive. Anyhow it follows from Table 1 that experimental points with low values of r_a require a steeper slope of eq. (5) in order to be fitted.

Table 1. Values of the slope of $E'(T_s)$ - eq. (6) - for different values of the aerodynamic resistance r_a

r_a		$-D_{T_s} E$
(day.cm ⁻¹)	(s.m ⁻¹)	(g.cm ⁻² .day ⁻¹ .K ⁻¹)
1.16	(1000)	.0212
.116	(100)	.0249
.0116	(10)	.0617

c. Variability of evaporation rate as related to the other meteorological variables

In Fig. 1 data of actual soil evaporation as obtained by the Bowen ratio method are plotted versus the corresponding surface temperatures.

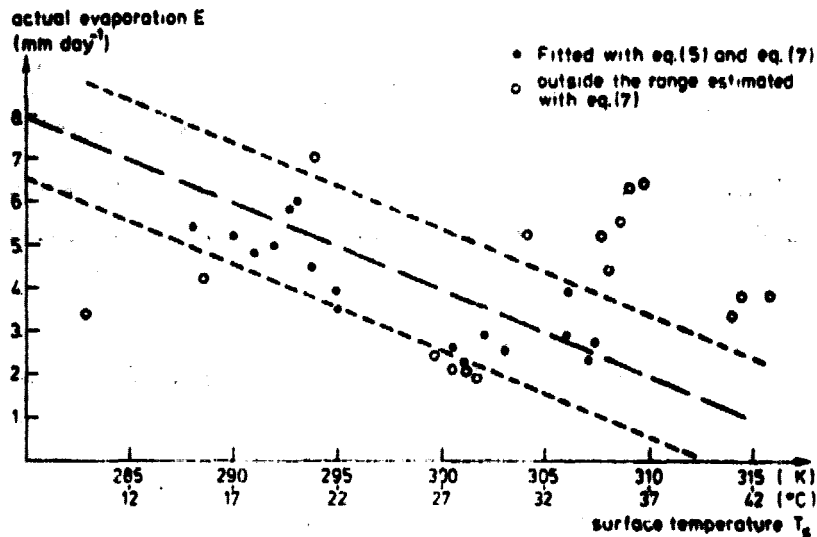


Fig. 1. Evaporation rates as calculated according to eq. (5) with a constant slope (middle broken line). The range of scatter due to surface albedo as calculated by eq. (7) is shown by the short broken lines. Measured evaporation rates E are plotted versus measured averaged daily surface temperature T_s . Dotted points are within, open circles are outside the range bounded by eq. (7)

The scatter due to differences in surface albedo is also shown, as evaluated from:

$$D_{\alpha} E = - \frac{R_s}{L} d\alpha \quad (\text{g.cm}^{-2}.\text{day}^{-1}) \quad (7)$$

and evaluated with $\delta\alpha = (\alpha_x - \alpha_N)/2$, corresponding to a $\delta_{\alpha} E = \pm 1.4 \text{ mm.day}^{-1}$, where α_x and α_N are the maximum (0.583) resp. the minimum value (0.262) of the surface reflectivity in the data set.

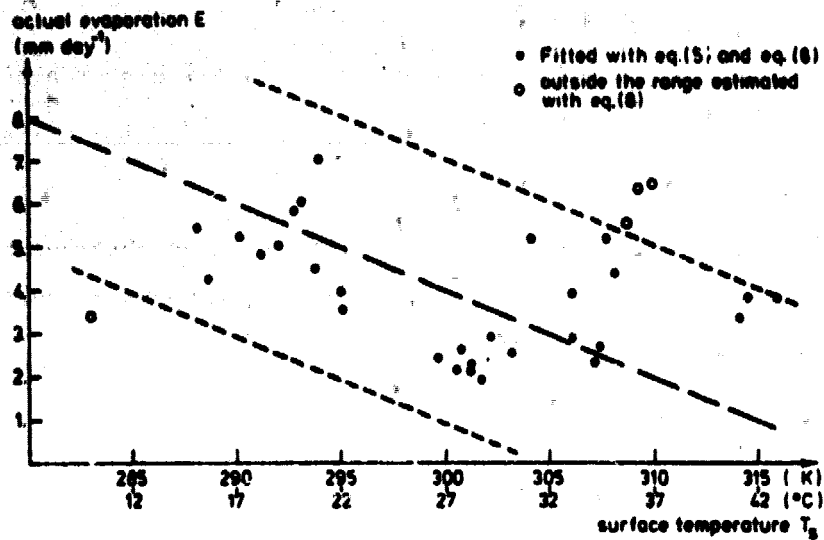


Fig. 2. As Fig. 1, but the range of scatter is not only due to surface albedo but also due to air temperature as calculated by eq. (8)

In Fig. 2 the scatter due to the air temperature, according to the derivative:

$$D_{T_a} E = \frac{1}{L} \left(4 \epsilon' \sigma T_a^3 - \frac{\rho_a c}{r_a} \right) d T_a \quad (\text{g.cm}^{-2} \cdot \text{day}^{-1}) \quad (8)$$

is also shown. In eq. (8) $\delta T_a = (T_a^x - T_a^N)/2$, where T_a^x and T_a^N are the maximum resp. the minimum value of air temperature in the data set. As can be seen from Fig. 2, this may account for a variability in evaporation of an additional $\pm 0.3 \text{ mm.day}^{-1}$. A comparison of Fig. 1 with Fig. 2 shows that the scatter due to the variability of surface reflectivity could be justified by a curve $E(T_s, \alpha)$.

Before continuing, the dependence of $D_{T_s} E$ on T_s must be evaluated. In the Figs. 3 and 4 $E(T_s)$ is calculated and plotted with a varying slope (eq. 5), while the scatter is calculated according to:

$$(\delta E)_{\max} = \frac{R_s \alpha^x - \alpha^N}{L} + \frac{4 \epsilon' \sigma \bar{T}_a^3}{L} \left(\frac{T_a^x - T_a^N}{2} \right) - \frac{\rho_a c}{L r_a} \left(\frac{T_a^x - T_a^N}{2} \right) \quad (\text{g.cm}^{-2} \cdot \text{day}^{-1}) \quad (9)$$

As can be seen, the results of Fig. 2 and Fig. 4 are practically equivalent.

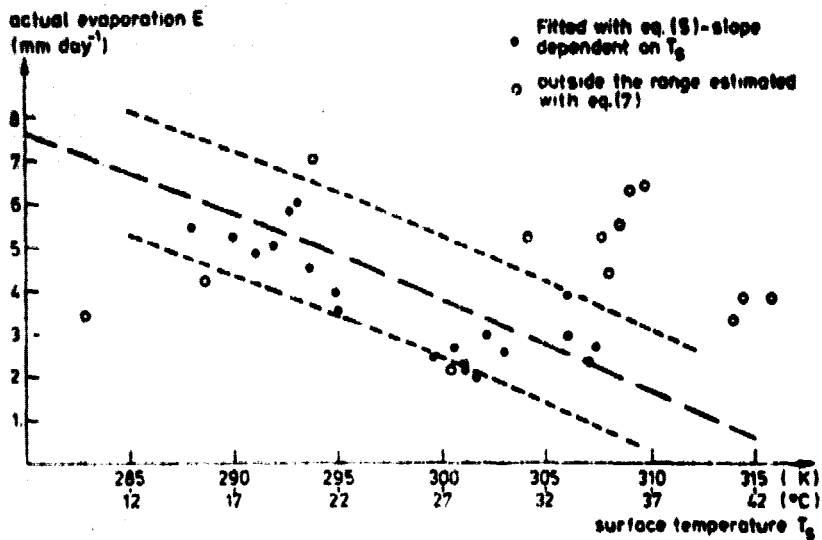


Fig. 3. As Fig. 1, but with the slope dependent on surface temperature

T_s

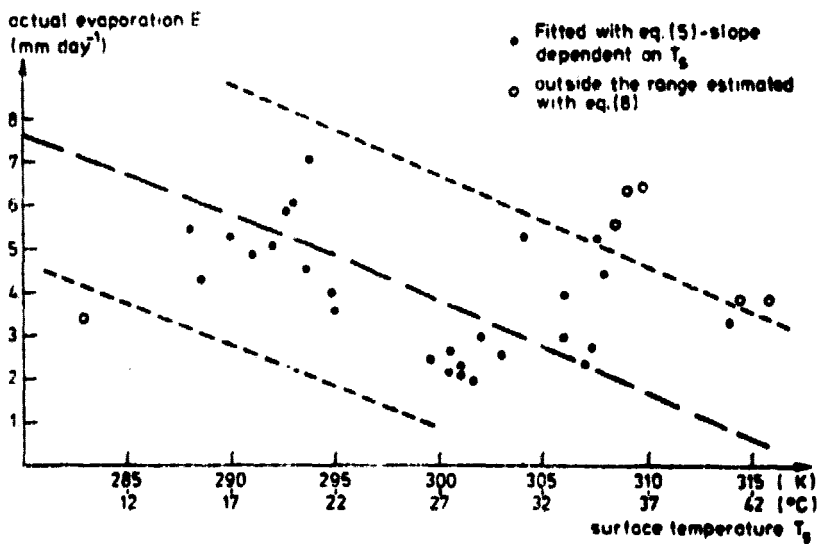


Fig. 4. As Fig. 2, but with the slope dependent on surface temperature

T_s

In a way similar to eq. (4), an analytical expression of $E(T_s, \alpha)$ can be derived:

$$E(T_s, \alpha) = \underline{E}(\underline{i}_8, \underline{i}_1, \underline{i}_2) \quad (\text{g.cm}^{-2}.\text{day}^{-1}) \quad (10)$$

or

$$E(T_s, \alpha) = E^* + D_{T_s} E dT_s + D_{\alpha} E d\alpha \quad (\text{g.cm}^{-2}.\text{day}^{-1}) \quad (11)$$

d. Numerical calculation of the derivative with respect to surface temperature and reflectivity

Eq. (11) can be written as:

$$E(T_s, \alpha) = E^* - \frac{1}{L} \left(\frac{\rho_a c_a}{r_a} dT_s + 4 \epsilon \sigma T_s^3 dT_s + R_s d\alpha \right) \quad (\text{g.cm}^{-2}.\text{day}^{-1}) \quad (12)$$

This equation corresponds to eq. (6) and, according to the same procedure applied there, the zeros of the second term of the right hand side of eq. (12) can be evaluated:

$$\frac{\rho_a c_a}{r_a} dT_s + 4 \epsilon \sigma T_s^3 dT_s + R_s d\alpha = 0 \quad (\text{J.cm}^{-2}.\text{day}^{-1}) \quad (13)$$

Solutions T_s'' of eq. (13) depend on the combination of the increments δT_s and $\delta \alpha$. In Table 2, values T_s'' are shown as included in the interval corresponding to the different values of r_a (Table 1). The left hand side of eq. (13) can be < 0 when either δT_s or $\delta \alpha$ is negative, according to the value of r_a . The headings of rows and columns in Table 2 show the different choices of δT_s and $\delta \alpha$.

For a proper interpretation of these results it must be kept in mind that they have been derived by Taylor's expansion of eq. (1). Thus the trend of the evaporation rate E is, strictly speaking, determined only in the neighbourhood of the point one is dealing with.

After collecting experimental values of the evaporation rate for different surfaces and periods one by one, the procedure to be applied is the following. Firstly one checks for a point P_1 if $D_{T_s, \alpha} E|_{P_1} < 0$ or > 0 . Secondly, for the points $P_1 \rightarrow P_2$ if $\delta_{T_s, \alpha} E|_{P_1} < 0$ or > 0 . This means to check if the points P_1 and P_2 can be P_1 connected by a monotonic single-value function of the couples (T_s, α) . The points P_1 and P_2 constitute a data set denoted S^2 . Then the same procedure is applied to a certain point P_3 looking for the nearest point in S^2 with respect to the coordinate system T_s, α . Now one has to check if

Table 2. Surface temperatures T_s'' (K) satisfying eq. (13) for different choices of δT_s and $\delta \alpha$, with $0.0116 \leq r_a \leq 1.16$ ($\text{day} \cdot \text{cm}^{-1}$).

When $\delta T_s < 0$, $E > E'$ for $T_s'' > T_s'$. The reverse holds for $\delta T_s > 0$

	$\delta \alpha = .1$		$\delta \alpha = -.1$	
	K	($^{\circ}\text{C}$)	K	($^{\circ}\text{C}$)
$\delta T_s = 1$	$-553 < T_s'' < -488$	$(-826 < T_s'' < -761)$	$396 < T_s'' < 386$	$(123 < T_s'' < 213)$
$\delta T_s = -1$	$396 < T_s'' < 486$	$(123 < T_s'' < 213)$	$-553 < T_s'' < -488$	$(-826 < T_s'' < -761)$
$\delta T_s = 5$	$-424 < T_s'' < -287$	$(-697 < T_s'' < 560)$	$-311 < T_s'' < 283$	$(-584 < T_s'' < 10)$
$\delta T_s = -5$	$-311 < T_s'' < 283$	$(-584 < T_s'' < 10)$	$-424 < T_s'' < -287$	$(-697 < T_s'' < 560)$

P_3 can be connected to its nearest point in S^2 with a slope of the same sign as in S^2 . If so, add P_3 to S^2 to get S^3 . If not, add P_3 to a second data sub-set where the slope is of opposite sign. Then repeat the procedure for each P_k with respect to S^{k-1} . Then it is possible to fit independently the two sets with positive ($\delta_{T_s, \alpha} > 0$) and negative ($\delta_{T_s, \alpha} < 0$) variation.

In the following, different relationships between E , T_s , α will be analytically derived and fitted to data obtained from a series of experiments performed in an inhomogeneous desert area.

e. First-order approximation of the surface $E(T_s, \alpha)$

In the present case the well known condition for four points belonging to the same plane leads to the following expression of the linear function $E'(T_s, \alpha)$:

$$\begin{vmatrix} T_s^1 - T_s^1 & \alpha - \alpha^1 & E - E^1 \\ T_s^1 - T_s^2 & \alpha^1 - \alpha^2 & E^1 - E^2 \\ T_s^3 - T_s^2 & \alpha^3 - \alpha^2 & E^3 - E^2 \end{vmatrix} = 0 \quad (14)$$

The points $P_1 \equiv (T_s^1, \alpha^1, E^1)$, $P_2 \equiv (T_s^2, \alpha^2, E^2)$, $P_3 \equiv (T_s^3, \alpha^3, E^3)$ must be chosen on the basis of eq. (1). This means that, with a minimal quantity of data, the Figs. 1 to 4 together with eq. (1) can be used to choose the points P_1, P_2, P_3 . The terms $E_{i_7 \cdot i_1}$ and $E_{i_7 \cdot i_2}$ in eq. (10) can be represented on the coordinate planes (E, T_s) and (E, α) respectively. If a constant value for $D_{T_s} E$ is used, $E'(T_s)$ and $E'(\alpha)$ are straight lines in the two planes. Evaluation of the slope of $E'(\alpha)$ requires an estimation of the shortwave incoming radiation. In this paper the average R_s of the whole data set (winter time and summer time data) is used. Evaluation of the slope of $E'(T_s)$ is more cumbersome, because $D_{T_s} E = f(T_s, r_a)$. As can be seen from Figs. 3 and 4, $D_{T_s} E$ is not varying strongly in the interval $280 < T_s < 320$ (K) ($7 < T_s < 47$ °C). As far as r_a is concerned, there is a strong variation of r_a in the existing data set. This problem will be discussed later in detail in section III.c. Anyhow, in order to evaluate the feasibility of very simple formulas (as derived in a formal way from the energy balance equation) only mean values are used.

III. NUMERICAL DEVELOPMENT OF LINEAR EVAPORATION EQUATIONS

a. Selection of suitable experimental points

Whether or not the use of eq. (14) is successful depends on the selection of the points P_1, P_2, P_3 (section II.e). The most reasonable choice seems to use extreme values either for T_s or α . One of the points P_i can be on the axis E, the other two on the coordinate planes (E, T_s) and (E, α) . With this solution it is likely that the experimental values of E are closer to the plane $E'(T_s, \alpha)$. The first step is to calculate the intercepts of the straight lines $E'(T_s)$ and $E'(\alpha)$ from eq. (5) and (7). When using the input data presented in Table 3, the following values for the derivatives are found:

$$D_{T_s} E = -0.206 \quad (\text{mm.day}^{-1} \cdot \text{K}^{-1}) \quad D_{\alpha} E = -8.86 \quad (\text{mm.day}^{-1}) \quad (15)$$

Table 3. Numerical input data used for the calculation of the functions $E'(T_g)$ and $E'(\alpha)$

Parameter	Value	Units
$\rho_a c_a$	1.154	$J.cm^{-3}.K^{-1}$
$4 \epsilon \sigma$	$18.615.10^{-7}$	$J.cm^{-2}.day^{-1}.K^{-4}$
\bar{r}_a	2.15	$day.cm^{-1}$
\bar{T}_s	300.8	K
\bar{R}_s	2154.8	$J.cm^{-2}.day^{-1}$
L	2432.3	$J.g^{-1}$ (at 27°C)

The functions $E'(\alpha)$, $E'(T_g)$ are described as:

$$E'(T_g) = -0.206 (T_g - 280) + m \quad (\text{mm.day}^{-1}) \quad (16a)$$

$$E'(\alpha) = -8.86 (\alpha - 0.25) + n \quad (\text{mm.day}^{-1}) \quad (16b)$$

The intercepts m and n can be calculated simply by imposing that two known points belong to the lines. The origin of the coordinate planes was chosen corresponding to $\alpha = 0.25$ and $T_g = 280^\circ K$, both values being smaller than the minimum values in the data set. The point $Q_1 \equiv (280, 0.362, 3.8)$ is on the plane (E, α) and the point $Q_2 \equiv (300.8, 0.25, 3.8)$ is on the plane (E, T_g) . The average values are: $\bar{E} = 3.8$, $\bar{T}_g = 300.8$, $\bar{\alpha} = 0.362$, and accordingly $m = 8.1$ and $n = 5.0$ were found. One of the three points required was chosen as $\bar{E} = (m+n)/2$. Then an arbitrary choice of the points $P(T_g, \alpha, E)$ can be:

$$P_1 \equiv (280., .25, 6.6); P_2 \equiv (300.8, .25, 4.); P_3 \equiv (280, .7, 1.2)$$

The point P_3 was also calculated from eq. (16b) on the plane (E, α) . From such a selection and according to eq. (14), a relationship between E , T_g and α was obtained as:

$$E'(T_g, \alpha) = -12.\alpha - 0.125 T_g + 44.6 \quad (\text{mm.day}^{-1}) \quad (17)$$

Since a poor agreement was obtained for experimental values cor-

responding to high reflectivities and low temperatures, a new trial was done with:

$$P_1 \equiv (280, .25, 6.6); P_2 \equiv (300.8, .25, 4.); P_3 \equiv (282.9, .583, 3.4)$$

where P_3 is measured. In this case the relationship obtained was:

$$E'(T_s, \alpha) = -8.52\alpha - 0.125T_s + 43.73 \quad (\text{mm.day}^{-1}) \quad (18)$$

b. Comparison between calculated and experimental values

The accuracy of eq. (18) and eq. (5) was tested against the experimental points of the Figures 1 to 4. In Table 4 measured E-data, estimated values $E'(T_s)$ from eq. (5) and $E'(T_s, \alpha)$ from eq. (18) are compared. Standard deviations are also shown. The experimental values were collected over quite different surfaces and different periods of the year.

Table 4. Comparison between experimental data with values obtained from eqs. (5) and (18)

E-function	Mean (mm.day ⁻¹)	σ (mm.day ⁻¹)
E	3.8	1.26
$E'(T_s)$ from eq. (5)	4.1	1.43
$E - E'(T_s)$	-.3	1.46
$E'(T_s, \alpha)$ from eq. (18)	3.2	1.21
$E_a - E'(T_s, \alpha)$	0.6	1.1

According to the theory developed in section II.d, it is still necessary to check the sign of the derivative for every point in the data set. Such a check was performed, with the derivatives evaluated using the average shortwave radiation \bar{R}_s , and the actual data of T_s and r_a . The aerodynamic resistance r_a was evaluated according to FEDES (1971) as:

$$r_a = \frac{e^* p_a}{p_a} [f(l) 1.15 u^{-.75}]^{-1} \quad (\text{s.m}^{-1}) \quad (19)$$

where e^* = ratio of molecular weight of water vapour to dry air

p_a = atmospheric pressure (pascal)

u = wind velocity (m.s^{-1})

$f(l) = a l^b$

l = height of roughness elements

$a = 0.167 \times 10^{-7}$ when $l \leq 20$ cm

$a = 0.3704 \times 10^{-7}$ when $l > 20$ cm

$b = .59$ when $l \leq 20$ cm

$b = .2827$ when $l > 20$ cm

The increments δT_s and $\delta \alpha$ were evaluated according to the procedure described in section II.d.

With such a procedure it was possible to separate the experimental points in two sub-sets, according to the negative and positive values of $D_{T_s, \alpha} E$. The sub-set with the positive derivative included five points out of the 33 presented in Figs. 1 to 4. A new evaluation of the accuracy of eq. (18) was performed for the sub-set with the negative derivative. Results are shown in Table 5.

Table 5. Comparison between experimental and calculated values of the sub-set with the negative derivatives

E-function	Mean (mm.day^{-1})	σ (mm.day^{-1})
E	3.6	1.25
$E'(T_s, \alpha)$	3.1	1.2
$E_a - E'(T_s, \alpha)$	0.5	1.1

The results of Table 5 are not excellent, but they still support the theory. In the following sections the effect of air temperature and the way how to handle data with very low r_a , will be analysed.

c. Effectiveness of the aerodynamic resistance, r_a

Up till now the dependence of E upon r_a was not taken into account. Such a hypothesis seems rather inaccurate because thus points of high aerodynamic resistance were connected with points of low aerodynamic resistance. From eq. (1) $D_{r_a} E$ is derived as:

$$D_{r_a} E = \frac{1}{L} \rho_a c_a (T_a - T_s) \frac{1}{r_a^2} d r_a \quad (\text{g.cm}^{-2}.\text{day}^{-1}) \quad (20)$$

Since a finite evaluation of $\delta_{r_a} E$ is needed, it is better to write eq. (20) as:

$$\delta_{r_a} E \left|_{P_i}^{P_j} = \frac{1}{L} \rho_a c_a \overline{(T_a - T_s)} \int_{P_i}^{P_j} \frac{1}{r_a^2} d r_a \quad (\text{g.cm}^{-2}.\text{day}^{-1}) \quad (21)$$

where P_i, P_j are points in the data set, and the average $\overline{(T_a - T_s)}$ is taken between P_i and P_j . The correction according to eq. (21) must be evaluated for the points in the data sub-set where $D_{T_s, \alpha} < 0$, for those points showing the highest roughness. The points to be considered together with the data required for the calculation are depicted in Table 6.

Table 6. Experimental input data corresponding to days and sites with low aerodynamic resistances r_a . The last column represents data obtained from calculations with eq. (18)

	T_s (K)	T_a (K)	α	r_a (day.cm ⁻¹)	E (mm.day ⁻¹)	$E'(T_s, \alpha)$ (mm.day ⁻¹)
1	308.7	305.7	0.298	0.11	5.5	3.58
2	309.2	312.7	0.301	0.11	6.3	3.54
3	309.9	310.3	0.303	0.13	6.4	3.50
4	307.9	306.2	0.304	0.07	5.2	3.56

Until now the relationship between actual evaporation rate E and surface characteristics T_s and α has been sought in a three-dimensional space (E, T_s, α). In principle evaluation of the effectiveness of r_a on E (without shadowing contributions from T_s and α) requires couples of points differing from each other only with respect to r_a . It is impossible to match with the data available such a constraint. Then points with almost the same value of T_s , but with different albedos were selected from the data-set. The data for these points are given in Table 7.

Table 7. Experimental input data corresponding to days and sites with T_s and α -data similar to those in table 6, but with high aerodynamic resistances, r_a . The last column again computed with eq. (18)

	T_s (K)	T_a (K)	α	r_a (day.cm ⁻¹)	E (mm.day ⁻¹)	$E'(T_s, \alpha)$ (mm.day ⁻¹)
1	308.2	308	0.477	2.33	4.4	2.09
2	307.2	309.4	0.422	2.68	2.3	2.58
3	307.6	309.8	0.442	2.43	2.7	2.4

It must be emphasized that the term $\delta_{r_a} E$ (eq. 21) is independent from the formulation given by eq. (18). Therefore taking care of the sign, the variation $\delta_{r_a} E$ must be added to the values of the column headed $E'(T_s, \alpha)$. According to eq. (21) the variations $\delta_{r_a} E$ between each separate point in Table 6 in combination with all the points of Table 7 were calculated. Results are shown in Table 8. From Table 8 it can be concluded that the calculation of $\delta_{r_a} E$ requires only approximate values of r_a . When r_a can be assigned to about 0.1 day.cm⁻¹ for a rough surface, and about 2 day.cm⁻¹ for a smooth one, $\delta_{r_a} E$ is determined sufficiently accurate. In Table 8 the row-index applies to the rows of Table 6 and the column-index to the rows of Table 7.

Table 8. Values of $\delta_{r_a} E$ (mm.day⁻¹) evaluated from Tables 6 and 7. The sign of $\delta_{r_a} E$ is for decreasing values of r_a .

	1	2	3	Average
1	1.65	1.5	1.5	1.55
2	0.9	0.9	0.9	0.9
3	1.0	1.0	1.0	1.0
4	3.5	3.3	3.05	3.3

For each row averages can be taken and can be used for estimation of corrections for differences in r_a .

Similar calculations as performed for Table 5 yield the results shown in Table 9. Improvement in the estimation of E is evident when comparing the standard deviations of E and $E - [E'(T_{s,\alpha}) + \delta_{r_a} E]$. It is important to recall that, unless Table 4, only those data were used with $D_{T_{s,\alpha}} < 0$.

Table 9. Comparison between experimental and calculated values. Eq. (18) corrected according to eq. (21)

E-function	Mean (mm.day ⁻¹)	σ (mm.day ⁻¹)
E	3.6	1.25
$E'(T_{s,\alpha}) + \delta_{r_a} E$	3.3	1.4
$E - [E'(T_{s,\alpha}) + \delta_{r_a} E]$	0.3	0.9

d. Effectiveness of air temperature

The results of Table 9 show that calculated values are rather close the measured data. However standard deviation is still too high. When looking at the data it seems that a systematic underestimation occurred during the period from 2 September to 8 September, 1978. This period was characterized by very high values of air temperature: the mean air temperature amounted to 35.8°C, while being 27.4°C over the

remaining data. Thus it was decided to evaluate an additional correction from eq. (8), using $\delta T_a = 8.4^\circ\text{C}$. Accordingly $\delta_{T_a} E = 1.8 \text{ mm.day}^{-1}$ was found. As for $\delta_{r_a} E$ the correction $\delta_{T_a} E$ is independent from the previous ones and must be added to $E'(T_s, \alpha)$. Applying such a correction yielded the results shown in Table 10.

Table 10. Comparison between experimental E and calculated (eq. 18) evaporation data with the corrections $\delta_{r_a} E$ (eq. 21) and $\delta_{T_a} E$ (eq. 8) being included

E-function	Mean (mm.day ⁻¹)	σ (mm.day ⁻¹)
E	3.6	1.25
$E'(T_s, \alpha) + \delta_{r_a} E + \delta_{T_a} E$	3.7	1.28
$E - [E'(T_s, \alpha) + \delta_{r_a} E + \delta_{T_a} E]$	-0.1	0.5

e. Summary of the results

Experimental values of actual evaporation rate, from different surfaces and periods, were compared with values calculated from eq. (18). Further corrections for the aerodynamic resistance r_a as obtained from eq. (21) and for the air temperature T_a as obtained from eq. (8) were applied (Table 10). The accuracy of the fit is also shown in Fig. 5, where measured versus calculated values are plotted. An interval equal to 2σ of $E_a - [E'(T_s, \alpha) + \delta_{r_a} E + \delta_{T_a} E]$ is also shown in Fig. 5.

In the evaluation of the corrections, the effect of atmospheric instability was not taken into account. However such an effect may be very important as far as period 2/9-8/9 is concerned. In those days surface temperatures even higher than 60°C were observed. In these conditions strong buoyancy phenomena develop. For these reasons the evaluation of r_a by eq. (19) under unstable conditions might be unreliable.

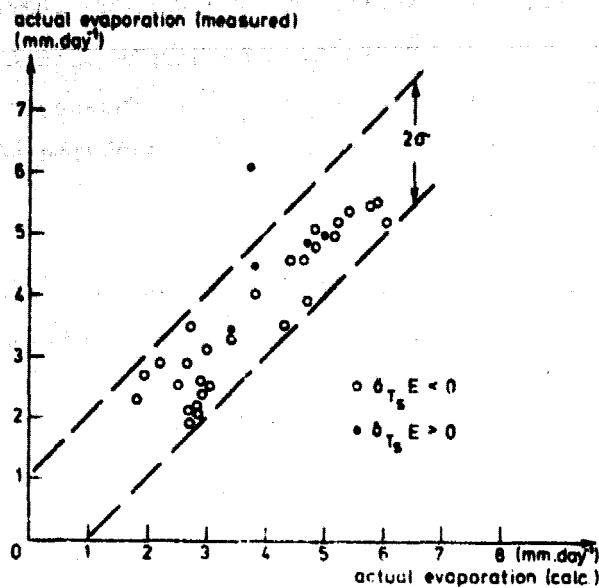


Fig. 5. Measured versus calculated (eq. 18) evaporation rates. Corrections included relate to surface aerodynamic resistance and air temperature. A scatter equal to twice the standard deviation is shown (broken lines)

IV. SUMMARY AND CONCLUSIONS

A simple procedure to evaluate actual evaporation has been derived by a geometrical representation of the energy balance equation, expressed as its first order Taylor's expansion. The role of the physical variables involved in the energy balance equation has been analysed. A linear relationship between actual evaporation and surface temperature was calculated and compared with experimental data. A bi-linear relationship between actual evaporation, surface temperature and albedo was also determined. Comparison with experimental data yielded promising results.

Corrections were applied as related to differences in aerodynamic resistance and air temperature for each day-experiment. The slope of the relationships between actual evaporation and surface characteristics

was shown to be strictly tied to aerodynamic resistance.

No relevant effect of the indetermination of the soil heat flux in desert dry soils was found.

After corrections were applied agreement between calculated and experimental evaporation data was shown to be good.

The formulas derived are oriented to applications involving remotely sensed surface temperature and albedo. The required basic data are: meteorological data, height and kind of soil coverage, mean value of the evaporation rate. These data allow the calculation of first-stage evaporation formulas. Short term experiments over different extreme situations were shown to be more useful than long-lasting experiments over a few surfaces.

The linear functions derived can be used for a straight forward evaluation of actual evaporation from MSS and IRLS data. These data provide the required values of surface temperature and albedo for each single area. The present procedure can be followed as a scheme, when evaluating evaporation losses from large inhomogeneous areas.

ACKNOWLEDGEMENTS

The results of the present paper are based on experiments performed in the Libyan desert. The author is indebted to the Libyan authorities and to AQUATER spA for permission to use these data.

The author is mostly grateful to the International Agricultural Center (IAC), the Institute for Land and Water Management Research (ICW) and TECNECO spA for making his 8 month's stay in Wageningen possible.

The author gratefully remembers his fruitful discussions on the matter with drs. R. Lupini and drs. E. Aliverti.

He specially acknowledges dr. R.A. Feddes for supervising the research and for revising the manuscript.

REFERENCES

- FEDDES, R.A. 1971. Water heat and crop growth. Thesis Comm. Agric. Univ., Wageningen 71-12. 184 pp.
- IDSO, S.B. et al., 1975. The dependence of bare soil albedo on soil water content. J. of Applied Met., vol. 14 no. 1: 109-113.
- JACKSON, R.D. et al., 1976. Calculation of evaporation rates during the transition from energy-limiting to soil-limiting phases using albedo-data. Water Res. Research, vol. 12 no. 1: 23-26.
- McCUEEN, R.H., 1974. A sensitivity and error analysis of procedures used for estimating evaporation. Water Resources Bull., vol. 10 no. 3: 486-497.
- REGINATO, R.J. et al., 1976. Soil water content and evaporation determined by thermal parameters obtained from ground-based and remote measurements. Journ. of Geophys. Res., vol. 81 no. 9: 1617-1620.
- SCHMUGGE, T. et al., 1978. Soil moisture sensing with aircraft observations of the diurnal range of surface temperature. Water Resources Bull., vol. 14 no. 1: 169-178.
- SEGUIN, B. 1973. Rugosité du paysage et évapotranspiration potentielle à l'échelle régionale. Agric. Met., vol. 11: 79-98.
- SOER, G.J.R. 1977. Estimation of regional evapotranspiration and soil moisture conditions, using remotely sensed crop surface temperatures. NIWARS publ. 45, Delft, the Netherlands. 30 pp.

LIST OF USED SYMBOLS

<u>Symbol</u>	<u>Interpretation</u>	<u>Units</u>
α	surface reflectivity	-
E	evaporation rate	$\text{g.cm}^{-2}.\text{day}^{-1}$
$E(T_s, \alpha)$	evaporation rate calculated as an arbitrary function of T_s, α	$\text{g.cm}^{-2}.\text{day}^{-1}$
$E'(T_s, \alpha)$	evaporation rate calculated as a linear function of T_s, α	mm.day^{-1}
ϵ	surface emissivity	
ϵ'	air apparent emissivity	
ϵ^*	ratio of molecular weight of water vapour to dry air	
G	soil heat flux	$\text{J.cm}^{-2}.\text{day}^{-1}$
l	height of roughness elements	cm
L	latent heat of vaporization of water	J.g^{-1}
p_a	atmospheric pressure	Pa
$\rho_a c_a$	thermal capacity of air	$\text{J.cm}^{-3}.\text{K}^{-1}$
r_a	surface aerodynamic resistance	day.cm^{-1}
R_s	shortwave incoming radiation	$\text{J.cm}^{-2}.\text{day}^{-1}$
σ	Stephan-Boltzmann constant	$\text{J.cm}^{-2}.\text{day}^{-1}.\text{K}^{-4}$
T_a	air temperature	K
T_s	surface temperature	K
$D_{x_i} E(x_1, \dots, x_n)$	partial derivative of E with respect to x_i . E is any function of (x_1, \dots, x_n)	
$\delta_{x_i} E(x_1, \dots, x_n)$	finite variation of E with respect to x_i . E is any function of (x_1, \dots, x_n)	